Ocotea daphnifolia: phytochemical investigation, in vitro dual cholinesterase inhibition, and molecular docking studies

Raquel Bianca Marchesine de Almeida[1,] Rodrigo Souza Conceição[1],
Kryzia Santana da Silva[2], Manoelito Coelho dos Santos Junior[2],
Alexsandro Branco[3]; Mariana Borges Botura [1]*

[1]Toxicology Laboratory, Department of Health, State University of Feira de Santana, Bahia, Brazil, [2]Molecular Modeling Laboratory, Department of Health, State University of Feira de Santana, Bahia, Brazil [3]Phytochemistry Laboratory, Department of Health, State University of Feira de Santana, Bahia, Brazil

This study aimed to evaluate the anticholinesterase activities of extracts and fractions of *Ocotea daphnifolia in vitro* and characterize its constituents. The effects of hexane, ethyl acetate, and ethanolic extracts on acetylcholinesterase (AChE) and butyrylcholinesterase (BuChE) activity were determined with a spectrophotometry assay. All extracts inhibited cholinesterase activity, and the ethanolic extract (2 mg/mL) exhibited the highest inhibition of both enzymes (99.7% for BuChE and 82.4% for AChE). The ethanolic extract was fractionated by column chromatography resulting in 14 fractions that were also screened for their anticholinesterase effects. Fraction 9 (2 mg/mL) showed the highest activity, inhibiting AChE and BuChE by 71.8% and 90.2%, respectively. This fraction was analyzed by high-performance liquid chromatography high-resolution mass spectrometry which allowed the characterization of seven glycosylated flavonoids (containing kaempferol and quercetin nucleus) and one alkaloid (reticuline). In order to better understand the enzyme-inhibitor interaction of the reticuline toward cholinesterase, molecular modeling studies were performed. Reticuline targeted the catalytic activity site of the enzymes. *Ocotea daphnifolia* exhibits a dual cholinesterase inhibitory activity and displays the same pattern of intermolecular interactions as described in the literature. The alkaloid reticuline can be considered as an important bioactive constituent of this plant.

Keywords: *Ocotea*. Acetylcholinesterase. Butyrylcholinesterase. Alkaloid. Flavonoid.

INTRODUCTION

Alzheimer's disease (AD), a chronic neurodegenerative disorder, is characterized by dementia, memory loss, and cognitive impairment. Several factors are associated with the pathology of AD, such as low levels of acetylcholine, β-amyloid (Aβ) deposits, oxidative stress, and tau protein hyperphosphorylation (Reid, Chilukuri, Darvesh, 2015). The main strategy in the clinical treatment of AD is based on the cholinergic hypothesis that

associates cognitive decline with a loss of acetylcholine (ACh). Cholinesterase inhibitors improve cholinergic activity in the brain of AD patients since they increase the availability of ACh in the synaptic cleft (Ahmed *et al.*, 2013).

There are two types of cholinesterases (ChE) responsible for the hydrolysis of ACh: acetylcholinesterase (AChE) and butyrylcholinesterase (BuChE). In a healthy brain, AChE is the most important enzyme that regulates the level of ACh, while BuChE plays a secondary role. However, in patients with AD, the level of AChE gradually declines, and the activity of BuChE increases with disease progression (Ahmed *et al.*, 2013). Moreover, BuChE may also participate in the formation of Aβ plaques (Reid,

Chilukuri, Darvesh, 2015). The dual inhibition of AChE and BuChE is a valuable approach and may provide additional benefits in the treatment of AD. The FDA has approved four AChE inhibitors (donepezil, galantamine, rivastigmine, and tacrine), and only these two last drugs act upon the two cholinesterases. These drugs can be used in the diagnosis or treatment of other diseases, such as myasthenia gravis, postoperative ileus, bladder distension, glaucoma, and cholinergic antidote (Colovic *et al.*, 2013). The high cost and serious side effects of many synthetic drugs have encouraged researchers to identify effective AChE and BuChE inhibitors in natural products with low toxicity.

Some plant secondary metabolites have been shown to effectively inhibit cholinesterases (Othman *et al.*, 2016). *Ocotea* is a genus that includes trees and shrubs and has the largest number of medicinal species of the Lauraceae family. Chemical investigations in several species of Ocotea have led to the isolation of a variety of secondary metabolites, such as alkaloids, lignans, flavonoids, and sesquiterpenes (Salleh, Ahmad, 2017). *Ocotea daphnifolia* (Meisn.) Mez is a tree found in different parts of Brazil, and no scientific information regarding its chemistry or biological activities has been reported so far. This study aimed to evaluate the AChE and BuChE inhibitory activities of extracts and fractions of *O. daphnifolia* leaves *in vitro* and to characterize the active chemical constituents present in this species. Additionally, molecular docking studies of *O. daphnifolia* alkaloids were performed to investigate the intermolecular interactions inside the cholinesterase active sites.

MATERIAL AND METHODS

Reagents and chemicals

Ethyl acetate, *n*-hexane, ethanol, methanol (analytical grade) and silica gel 60 (70–230 mesh) were obtained from VETEC. The substances used for the anticholinesterase test, acetylthiocholine iodide (ATCI), 5,5′-dithiobis(2-nitrobenzoic-acid) (DTNB), S-butyrylthiocholine chloride (BTCI), physostigmine, acetylcholinesterase from *Electrophorus electricus* (EC 3.1.1.7, Type VI-S) and butyrylcholinesterase from equine serum (EC 3.1.1.8) were obtained from Sigma-Aldrich® (St. Louis, MO, USA). Sodium phosphate dibasic and sodium phosphate monobasic were obtained from Anidrol (Diadema, SP, Brazil).

Plant material

Leaves of *O. daphnifolia* (Meisn.) Mez were collected in the municipality of Rio de Contas (Bahia) in December 2013. The identification of the plant species was conducted by a botanist and a voucher specimen (HUPES 205862) was deposited at the herbarium of the State University of Feira de Santana, Brazil.

Obtainment of the extract

Around 1.04 kg of dried and ground *O. daphnifolia* underwent successive extraction by maceration for 72 h using solvents of increasing polarity (hexane, ethyl acetate, and ethanol). After filtration, a solvent removal step was performed by evaporation using a rotary evaporator according to standard methodologies for plant extraction (Tachakittirungrod, Okonogi, Chowwanapoonpohn, 2007). The extraction process yielded the hexane extract (7.83 g, 0.75%, HE), ethyl acetate extract (16.49 g, 1.6%, EAE), and ethanol extract (36.28 g, 3.5%, EE).

Fractionation of the active extract

About 24.16 g of the crude ethanol extract was fractioned in column chromatography (CC), with solvents in the order of increasing polarity (hexane, ethyl acetate, and ethanol) resulting in 14 fractions (F1-F14). All fractions were then screened for cholinesterase enzyme inhibitory activity *in vitro*.

HPLC-HRMS/MS analysis

The fraction with greater activity was analyzed through high-performance liquid chromatography high-resolution mass spectrometry (HPLC-HRMS/MS), Amazon Speed ETD model and APCI adapter, positive mode in the analytical center of the Chemistry Institute at the Federal University of Sao Paulo. The chromatograph used was Shimadzu, containing the column Luna C18 (250 mm x 4.6 mm, 5 μm). The mobile phase system corresponded to (A) H_2O/acetic acid 0.1% and (B) methanol, and the gradients were as follows: time 0-20 min, linear gradient from 5% to 100% B; 20-24 min, isocratic 100% B; 24-25 min, linear gradient from 100 to 5% B; and 25-35 min, isocratic 5% B. The flow of the mobile phase and the oven temperature were 1.0 mL/min and 40 °C, respectively.

In vitro cholinesterase inhibitory activity

AChE inhibitory activity was evaluated using Ellman's microplate assay, with a few modifications, as described by Tan *et al.* (2014) using AChE from *E. electricus*. The extracts and fractions were evaluated at different concentrations ranging from 0.25 to 2.0 mg/mL. Briefly, 0.1 M sodium phosphate buffer containing bovine serum albumin (140 µL), extracts/fractions (20 µL), and an enzyme solution (0.15 U/mL, 20 µL) were homogenized (microplate reader) and incubated at room temperature for 30 min. Then, 10 µL of 10 mM DTNB were added into each well, followed by the addition of acetylthiocholine iodide (14 mM, 10 µL). Positive (eserine 14 µg/mL) and negative controls (1% ethanol and 0.1 M phosphate buffer) were also included. The absorbance was measured at 405 nm in a Multiskan microplate reader (Thermo Scientific ®) at 0 and 30 min. For the BuChE inhibitory assay, the same procedure was followed except that the enzyme and substrate used were BuChE (0.15 U/mL) from the equine serum and S-butyrylthiocholine chloride (14 mM), respectively. The percentage of the enzymatic activity was calculated using the following formula: % Inhibition = {1 - [(T30 - T0 sample) / (T30 - T0 CN / TF)]} × 100 (where T0 is the absorbance reading after the start of the reaction; T30, the absorbance reading at 30 min after T0; CN, negative control; and TF, phosphate buffer).

Molecular docking

Molecular docking was performed for alkaloid identified in the most active fraction (reticuline) through DOCK 6.7 programs and accessories. The chemical structures of reticuline were named as R-1, R-2, R-3, and R-4 (Figure 1). The preparation of these molecules was performed in Chimera 1.9 with the calculation of Gasteiger-Hückel charge and the addition of polar hydrogens. Crystallographic structures of cholinesterases were obtained from the Protein Data Bank (PDB) [PDB ID: 6O4W (Gerlits *et al.*, 2019) and PDB ID: 4AQD (Brazzolotto *et al.*, 2012) for AChE (complexed with donepezil) and BuChE (complexed with tacrine), respectively. 6O4W and 4AQD structures were processed with the Dock Prep module in Chimera 1.9. The solvent access of the molecular surface of the enzymes was calculated with DMS accessory software (Ferrin *et al.*, 1988). The negative image of the molecular surface was generated as a set of superimposed spheres through SPHGEN software (Kuntz *et al.*, 1982). The file was edited by SPHERE SELECTOR (Kuntz *et al.*, 1982) to contain only the spheres with a distance of 8.0 Å from the crystallographic ligand. The box around each active site was built with SHOWBOX accessory software. The delimitation of the active site was performed according to the position of the co-crystallized ligand with the respective protein (AChE and BuChE). The grids were computed with GRID accessory software based on the following parameters: attractive distance of energy = 6.0 Å, repulsive distance from van der Waals force = 9.0 Å, and overlap crash = 0.75 Å (Shoichet, Kuntz, Bodian, 1992). Ligands were minimized utilizing a simplex algorithm implemented in DOCK 6.7 (Nelder, Mead, 1965). The GridScore score function was used for the classification of the affinity energy between molecules with enzymes. The docking success was measured by calculating the root mean square deviation (RMSD) of the docking pose against its conformation in the crystal structure. An RMSD lower than 2 Å is considered a very good result (Yang, Roy, Zhang, 2013). The complexes formed were selected according to the value of the scoring function, and the intermolecular interactions were analyzed using the Protein-Ligand Interaction Profiler.

FIGURE 1 - Chemical structures of (S) -reticuline used in molecular docking

Statistical analysis

Data are expressed as the mean ± SD. Statistical analysis was performed using a one-way analysis of variance followed by Tukey's test (5%). Differences were considered significant at p<0.05. The IC_{50} of the active extract and fraction were calculated through nonlinear regression analysis. All statistical analyses were performed using the GraphPrism statistical program (version 5.0).

RESULTS AND DISCUSSION

In vitro cholinesterase inhibitory activity

All extracts of *O. daphnifolia* showed a concentration-dependent anticholinesterase activity on the enzymes AChE and BuChE. The EE was the most active, and all the evaluated concentrations presented a statistically significant difference in relation to the negative control (p<0.001). The mean percentage inhibitions of EE at the highest concentration tested (2 mg/mL) for AChE and BuChE were 82.4% and 99.7%, respectively. The lowest anticholinesterase effect was observed for EAE (AChE, 20.4%; BuChE, 66.9%) and HE (AChE, 46.2%; BuChE, 86.4%) (Figure 2). Only for the EE in the BuChE assay was it possible to calculate the IC_{50}, which was 0.59 mg/mL (R^2 =0.98).
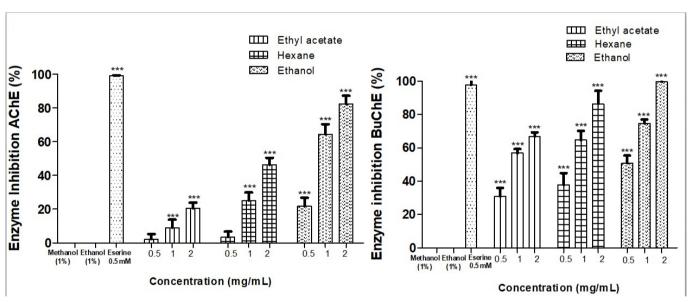

FIGURE 2 - Mean and standard deviation of the inhibition percentage of AChE and BuChE activities after treatment with the extracts of *O. daphnifolia*

A plant extract is considered a potent AChE inhibitor when it inhibits the enzyme by over 50% (Vinutha *et al.*, 2007). Considering this criterion, only the EE (1.0 mg/mL) was classified as potent inhibitor against AChE, while for BuChE, all extracts were potent, although at different concentrations: 0.5 mg/mL (EE) and 1.0 mg/mL (EAE and HE). The present work is the first to report the biological activity of *O. daphnifolia*. Previous studies demonstrated a similar effect on AChE activity of another Ocotea species, *Ocotea bullata* (Amoo *et al.*, 2012). However, no reports were found that describe the effects of plants of the genus Ocotea on BuChE.

Among the cholinesterases, BuChE was more sensitive to the effects of all extracts of *O. daphnifolia*. Similar results were reported in an anticholinesterase activity study with the *Rauvolfia reflexa* species. Differences in the structure of AChE and BuChE may interfere with the inhibitory effect of various compounds. Although cholinesterases exhibit a sequence identity above 50%, the internal volume of the active site of AChE is lower than that of BuChE (Fadaeinasab *et al.*, 2015).

The fractionation of the most active extract (ethanolic) yielded 14 fractions. All fractions significantly

inhibited the activity of both cholinesterases compared to the negative control (p< 0.001), except for the Fr1 and Fr4. Similar to the extracts, many of the fractions were more effective against BuChE. This increased inhibitory effect was observed for fractions 8, 9 and 10 that inhibited AChE by 70.1%, 71.8%, and 63.8% and BuChE by 87.8%, 90.2%, and 81.9%, respectively (Table I). For the most active fraction (Fr 9), it was possible to determine the IC_{50} against BuChE, which was 0.87 mg/mL ($R^2 = 0.99$).

The percent inhibition exhibited by these fractions was lower than those found for the EE (extract that yielded the fractions). These findings suggest a possible synergistic action of different compounds in the biological activity of *O. daphnifolia*. Plants produce a diversity of secondary metabolites, and their mode of action may be associated with synergistic interactions of the metabolites (Kaufmann *et al.*, 2016).

TABLE I - Mean and standard deviation of the inhibition of AChE and BuChE activities (%) after treatment with the fractions of the ethanolic extract of *O. daphnifolia*

Fraction (2 mg/mL)	AChE	BuChE
1	10.5 ± 4.3	0
2	23.9 ± 14.9***	27.7 ± 3.4***
3	23.8 ± 5.7***	25.5 ± 3.4***
4	9.4 ± 3.8	3.0 ± 3.7
5	47.8 ± 4.5***	32.0 ± 4.9***
6	39.0 ± 11.1***	36.5 ± 4.8***
7	46.2 ± 6.7***	47.1 ± 3.1***
8	70.1 ± 5.3***	87.8 ± 3.1***
9	71.8 ± 5.0***	90.2 ± 1.2***
10	63.8 ± 6.3***	81.9 ± 10.2***
11	45.4 ± 8.9***	31.0 ± 3.0***

(continuing)

TABLE I - Mean and standard deviation of the inhibition of AChE and BuChE activities (%) after treatment with the fractions of the ethanolic extract of *O. daphnifolia*

Fraction (2 mg/mL)	AChE	BuChE
12	46.4 ± 7.0 ***	31.8 ± 7.0***
13	29.2 ± 10.6***	30.6 ± 9.0***
14	22.7 ± 2.1***	68.1 ± 10.6***
Eserine (0.014 mg/mL)	98.8 ± 0.7***	99.3 ± 0.3***
(Ethanol 1%)	0±0	0±0

HPLC-HRMS/MS analysis

The HPLC-HRMS/MS chromatogram (positive mode) of the active fraction (Fr 9) isolated from the *O. daphnifolia* extract is shown in Figure 3. The mass spectra analysis of the peaks showed that the fraction contained mainly flavonol glycosides (peaks 2 to 8) and a minor proportion of alkaloids (peak 1). Table II shows the mass spectra of these flavonoid glycosides. The mass fragmentation showed the cleavage of interglycosidic bonds in position C-3, resulting in the formation of the intense flavonoid nucleus fragment (quercetin or kaempferol) (Gouveia-Figueira, Castilho, 2015). The mass spectra and a description of MS/MS fragmentation for each flavonoid structure (March *et al.*, 2006; Vukics, Guttman, 2008; Tsimogiannis *et al.*, 2007) can be found in the supplementary material.

Peak 2 showed a pseudo-molecular ion at *m/z* 627.1552 Da [M+H]+ and the aglycone signal at *m/z* 303.0513, suggesting the existence of quercetin as aglycone and two hexose moieties [M+H-162-162]+assigned to quercetin-3-*O*-hexose-hexoside. Peak 3 (*m/z* 597.1451 Da, [M+H]+) in the respective mass spectra showed the formation of the product ion relative to quercetin aglycone (*m/z* 303.0510), and it was classified as quercetin-3-*O*-hexose-pentoside. Peak 4 showed a molecular ion at *m/z* 567.1344 Da, and it was indicative of quercetin-3-*O*-dipentoside due to the loss of two pentoses. Peaks 6 and 7 showed pseudo-molecular ions at *m/z* 465.1030 Da and *m/z* 435.0925 Da, which can be associated with quercetin-3-*O*-hexoside

and quercetin-3-O-pentoside, respectively. Peaks 5 (m/z 581.1507 Da, [M+H$^+$]$^+$) and 8 (m/z 449.1084 Da, [M+H$^+$]$^+$) showed aglycone signals at m/z 287.0568 and 287.0577, with neutral losses of one pentose (-132) and one hexose

(-162), respectively. These compounds were identified as kaempferol-3-O-hexose-pentoside and kaempferol-3-O-hexoside (Gouveia-Figueira, Castilho, 2015; March, Miao, 2004).
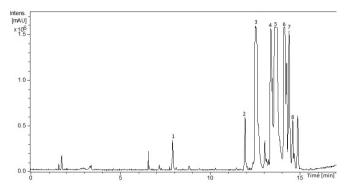

FIGURE 3 - HPLC-HRMS chromatogram of the total flavonol glycosylated ions

TABLE II - The flavonol glycosides of the *O. daphnifolia* ethanolic extract.

Peak	t_R (min)	[M+H$^+$]$^+$ (m/z)	MS^2	MS^3	Compound
2	12.0	627.1552	303.0513	257.0460, 229.0506, 201.0564, 187.0411	Quercetin-3-O-hexose-hexoside
3	12.5	597.1451	303.0510	257.0459, 229.0514, 201.0569, 187.0412	Quercetin-3-O-hexose-pentoside
4	13.4	567.1344	303.0513	257.0459, 229.0511, 201.0564	Quercetin-3-O-dipentoside
5	13.5	581.1507	287.0568	213.0563165.0208	Kaempferol-3-O-hexose-pentoside
6	13.8	465.1030	303.0512	257.0452, 229.0512, 201.0566	Quercetin-3-O-hexoside
7	14.0	435.0925	303.0516	257.0457, 229.0511, 201.0563	Quercetin 3-O-pentoside
8	14.4	449.1084	287.0577	258.0533, 213.0561, 165.0204	Kaempferol-3-O-hexoside

t_R: retention time; [M+H]$^+$: molecular ion; m/z: mass-to-charge ratio

In addition, peak 1 in the active fraction was identified as an alkaloid derivative (Figure 3). This compound peak showed a pseudo-molecular ion at m/z

330.1709 Da [M+H$^+$]$^+$ and fragments at m/z 192.1040 Da and m/z 177.0805 Da due to loss of two CH$_3$ radicals. These data were compatible with the alkaloid reticuline,

an aporphine alkaloid derived from a benzylisoquinolinic skeleton (Schmidt *et al.*, 2005). Similar fragment profiles were found (Yan *et al.*, 2013).

The benzylisoquinoline alkaloid reticuline, coclaurine and nacetylnorjuzifine were isolated from the bark and stem of the *Ocotea duckei* Vattimo (Morais, Barbosa-Filho, Almeida, 1998). The alkaloid class represents the main metabolites responsible for the anticholinesterase effects of plants. A study revealed high anticholinesterase activity of 9 alkaloids, including reticuline, against AChE and BuChE. These compounds presented a greater inhibition of BuChE in relation to AChE. These data were in agreement with the findings of the present study (Othman *et al.*, 2016).

Molecular docking

Molecular docking was performed with reticuline, the alkaloid found in the most active fraction of *O. daphnifolia*, to understand and compare its binding interaction with the cholinesterases: AChE (PDB ID: 6O4W) and BuChE (PDB ID: 4AQD). The molecular docking results were considered accurate because the RMSD value was below 2.0 Å (AChE: 1.33 Å; BuChE: 0.26 Å).

Figure 4 represents the map of reticuline intermolecular interactions with AChE. The molecular docking of reticuline (R-1) with AChE occurs through a hydrophobic interaction of the indole ring of the amino acid Trp279 with the junction of the A and B rings of reticuline. The hydroxyl, -OH, of the A-ring of the molecule forms hydrogen bonds with the amino acid residues Phe288 and Arg289. The methoxyl, -OCH3, carries out the same type of molecular interaction with the side chain of Tyr124. The methoxyl, -OCH3, of ring C forms two hydrogen bonds with both the amine group and the carboxylic group of the amino acid residue Ser286.

The chemical structure of reticuline depicted in R-2 exhibited hydrophobic interactions of its B and C rings with Trp86. The indole region of this residue performs a π-cation interaction with the B ring of the reticuline molecule. This residue participates in the acetylcholine binding site of mammalian AChE (Bennion *et al.*, 2015). The A ring performs a parallel π–π stacking interaction with Phe338 and parallel π–π stacking interaction with the Tyr337 phenol group, and that residue still binds hydrogen with the A ring -OH group. The protonated amine present in the B ring forms a Glu202 salt bridge and a His447 imidazole hydrogen bond. The Asp74 residue of AChE interacted by means a hydrogen bond with the -OH, and

-OCH3 groups of the C ring. The binding site of human AChE consists of the catalytic triad (Ser203, Glu334, and His447) which lies of the bottom of 20 Å deep and narrow binding gorge. The anionic domain binds the quaternary trimethylammonium choline moiety of Ach residues aromatic ones: Trp86, Tyr130, Tyr337, and Phe338. In human AChE, π-cation interactions with Trp86 are also observed (Atanasova *et al.*, 2015).
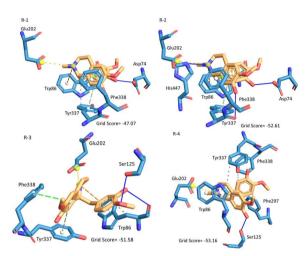

FIGURE 4 - Profile of intermolecular interactions of reticuline with AChE. Amino acids, blue; reticuline, orange; hydrogen bonds, blue solid line; hydrophobic interactions, dashed line ash; stacking-π type P (parallel), dashed lines light green; type T (perpendicular), dark green dashed lines. GridScore kcal/mol

The molecular docking of the reticuline molecule with the structure represented by R-3 showed two hydrophobic interactions of the C ring and the portion of the molecule that binds C and B to the side chain of Trp86. This type of intermolecular interaction is also found with this amino acid in R-2. The phenolic ring of Tyr330 interacts with the C ring of the compound through hydrophobic interactions. The -OH of the C and A rings binds hydrogen to the side chain of Ser125 and Tyr124, respectively. The tertiary amine

of the B ring performs an electrostatic interaction with the amino acid Glu202. The molecular docking of the reticuline molecule with the structure represented by R-3 showed hydrophobic interactions of the C ring and the portion of the molecule that binds C and B to the side chain of the Trp86. This type of intermolecular interaction was also found with this amino acid in R-2. The -OH and -OCH3 of the C ring bind hydrogen to the indole group of Trp86 and Ser125, respectively. The tertiary amine

of the B ring performs a salt bridge interaction with the amino acid Glu202 and Trp86 aromatic ring, performing a cation-π interaction with the B ring. The A ring interacts with π-stacking (parallel) and π-stacking (perpendicular) with Phe338 and Tyr337, respectively. It is observed that the amine group of reticuline, as in the anacardic acid studied, is an electron donor region capable of interacting with PAS residues (Kiametis *et al.*, 2017).

The A ring of the reticuline molecule in the conformation represented in R-4 showed a hydrophobic interaction with the Trp86 indole nucleus and a hydrogen bond with Ser125. In the B ring, there was a hydrophobic interaction with Trp86 and Tyr337. The C ring and Phe297 form a hydrophobic interaction, which also occurs with the Phe338 residue. Previous studies reported the interactions of known inhibitors (tacrine and galantamine) with Tyr337 and Trp86, which are residues present in the gorge of human AChE (Atanasova *et al.*, 2015; Khan *et al.*, 2018).

In Figure 5, the molecular conformations of reticuline are represented by the interactions carried out with the amino acids of BuChE. The R-1 conformation shows a hydrophobic interaction of the A ring with the indole ring of Trp79. The residue Trp79 is located in the region near the triad of BuChE (Ser195-His435-Glu322). This residue influences the mode of binding of all derivatives, participating in the orientation of the charges within the catalytic site. The -OH and -OCH3 groups attached to the A ring form a hydrogen bond with Thr117 and Tyr125, respectively. This ring forms two π-stacking parallel displaced interactions with Trp79. The C ring was stabilized by a hydrophobic interaction with Phe326 and through a hydrogen bond of its -OH group with Gly113. The B ring shows only a hydrophobic interaction with Trp79. The hydrophobic characteristics of the alkaloid in the R-2 conformation were similar to those found in R-1. Hydrophobic interactions play an important role in stabilizing ligand-receptor complexes. Only the -OH group of the A ring shows a hydrogen bond with Asp67, whereas the B ring amine forms a π-cation interaction with Trp79 and an ionic bond with Glu194. The Asp67 residue of BuChE is one of the most important residues because it is involved in controlling the architecture of the active site and the initial binding of the positively charged substrates (Nawaz *et al.*, 2011). The R-3 conformation was stabilized by hydrophobic interactions: B-Trp79 ring and C-Phe326 ring. The amine of the B ring interacts via a salt bridge with Glu194.
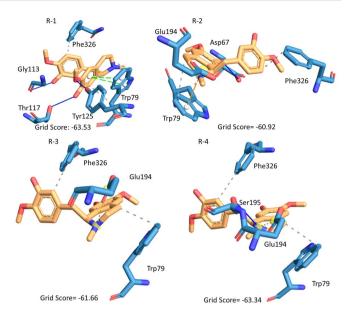

FIGURE 5 - Profile of intermolecular interactions of reticuline with BuChE. Amino acids, blue; reticuline, orange; hydrogen bonds, blue solid line; hydrophobic interactions, dashed line ash; Stacking-π type P (parallel), dashed lines light green; type T (perpendicular), dark green dashed lines. GridScore kcal/mol

The hydrophobic interactions of the molecule in the R-4 conformation presented the same pattern observed for R-3, differing only by the hydrogen bond in the B ring amine with Ser195. Molecular modeling studies show sequence alignment between equine BuChE and human BuChE (identity of 90%), and no differences were detected for the amino acid sequences within the active sites between the human and nonhuman sources (Bacalhau *et al.*, 2016). Previous studies described that 2-methoxyatherosperminine, a phenanthrene alkaloid, docked at the choline-binding site and catalytic triad of BuChE from *Homo sapiens* and showed a higher anticholinesterase effect *in vitro* against BuChE compared with AChE (Othman *et al.*, 2016). Ui-haq *et al.* (2010) suggest that the main differences between BuChE and AChE are related to residues present in the space of the enzymatic cavity. In AChE aromatic groups, they are replaced by more hydrophobic groups. Phe at the AChE acyl linkage site is replaced by Leu and Val residues, respectively. The pattern of reticuline interactions with BuChE was also been reported in docking studies with known ligands. Rivastigmine exhibited hydrophobic interactions with Trp residues and hydrogen bonds with Ser, Tyr, and Thr residues (Bacalhau *et al.*, 2016). Asp residues interact with cationic substrates, and Tyr has been

implicated in the binding of substrates and inhibitors to BuChE, suggesting that this amino acid residue is part of the P-site of this enzyme (Macdonald *et al.*, 2012). Different amino acid residues in the active site of BuChE, but not AChE, can accommodate compounds in their active site (Khaw *et al.*, 2014).

Another class of secondary metabolites found in the most active fraction of *O. daphnifolia* was glycosylated flavonoids derived from kaempferol and quercetin. *In silico* interactions of flavonoids and glycosylated flavonoids with AChE have already been investigated by Xie *et al.* (2014), who reported that the glycosylation decreases the AChE inhibitory activities of flavonoids (quercetin, baicalein, and myricetin).

Ocotea daphnifolia have a dual cholinesterase inhibitory activity and exhibited more affinity for BuChE. The most active fraction is characterized by the presence of the reticuline alkaloid and glycosylated phenolic compounds derive from the flavonoid kaempferol and quercetin.

The molecular docking technique generally utilizes an energy-based scoring function to obtain the most favorable ligand orientation and conformation required for binding at the active site (Jang *et al.*, 2018). The molecular docking of reticuline on AChE and BuChE suggested that this compound is capable of interacting with the catalytic activity site of both enzymes. The reticuline alkaloid is possibly an important bioactive constituent of the species *O. daphnifolia*.

ACKNOWLEDGMENTS

DISCLOSURE OF CONFLICTING INTERESTS

The authors declare that they have no conflict of interest.

REFERENCES

Ahmed F, Ghalib RM, Sasikala P, Ahmed KK. Cholinesterase inhibitors from botanicals. Pharmacogn Rev. 2013;7(14): 121–130.

Amoo SO, Aremu AO, Moyo M, Van Staden J. Antioxidant and acetylcholinesterase-inhibitory properties of long-term stored medicinal plants. BMC Complement Altern. 2012;12:1-9.

Atanasova M, Yordanov N, Dimitrov I, Berkov S, Doytchinova I. Molecular docking study on galantamine derivatives as cholinesterase inhibitors. Mol Inf. 2015;34:394-403.

Bacalhau P, San Juan AA, Goth A, Caldeira AT, Martins R, Burke AJ. Insights into (S)-rivastigmine inhibition of butyrylcholinesterase (BuChE): Molecular docking and saturation transfer difference NMR (STD-NMR). Bioorg Chem. 2016;67:105-109.

Bennion BJ, Essiz SG, Lau EY, Fattebert JL, Emigh A, Lightstone FC. A wrench in the works of human acetylcholinesterase: soman induced conformational changes revealed by molecular dynamics simulations. PLoS One. 2015;10(4):1-31.

Brazzolotto X, Wandhammer M, Ronco C, Trovaslet, M, Jean L, Lockridge O, et al. Human butyrylcholinesterase produced in insect cells: huprine-based affinity purification and crystal structure. The FEBS Journal. 2012;279(16):2905-2916.

Colovic MB, Krstić DZ, Lazarević-Pašti TD, Bondžić AM, Vasić VM. Acetylcholinesterase inhibitors: pharmacology and toxicology. Curr Neuropharmacol. 2013;11(3):315-335.

Fadaeinasab H, Basiri U, Kia Y, Karimian H, Ali HM, Murugaiyah V. New Indole alkaloids from the bark of *Rauvolfia reflexa* and their cholinesterase inhibitory activity. Cell Physiol Biochem. 2015;37(5):1997-2011.

Ferrin TE, Huang CC, Thomas E, Jarvis LE, Langridge R. The Midas display system. J Mol Graph Model. 1988;6(1):13–27.

Gerlits O, Ho KY, Cheng X, Blumenthal D, Taylor P, Kovalevsky A, et al. A new crystal form of human acetylcholinesterase for exploratory room-temperature crystallography studies. Chem Biol Interact. 2019;309:1-9.

Gouveia-Figueira SC, Castilho PC. Phenolic screening by HPLC-DAD-ESI/MS[n] and antioxidant capacity of leaves, flowers and berries of *Rubus grandifolius* Lowe. Ind Crops Prod. 2015;73:28–40.

Jang C, Yadav DK, Subedi L, Venkatesan R, Venkanna A, Afzal S, et al. Identification of novel acetylcholinesterase inhibitors designed by pharmacophore based virtual screening, molecular docking and bioassay. Nature Scientific Reports. 2018:8;1-21.

Kaufmann D, Dogra AK, Tahrani A, Herrmann F, Wink M. Extracts from traditional chinese medicinal plants inhibit acetylcholinesterase, a known alzheimer's disease target. Molecules. 2016;21(9):2-16.

Khan MB, Palaka BK, Sapam TD, Subbarao N, Ampasala DR. Screening and analysis of acetyl-cholinesterase (AChE) inhibitors in the context of Alzheimer's disease. Bioinformation. 2018;14(8):414–428.

Khaw KY, Choi SB, Tan SC, Wahab HA, Chan KL, Murugaiyah V. Prenylated xanthones from mangosteen as promising cholinesterase inhibitors and their molecular docking studies. Phytomedicine. 2014;21(11):1303-1309.

Kiametis AS, Silva MA, Romeiro LAS, Martins JBL, Gargano R. Potential acetylcholinesterase inhibitors: molecular docking, molecular dynamics, and *in silico* prediction. J Mol Model. 2017;67:1-10.

Kuntz ID, Blaney JM, Oatley SJ, Langridge R, Ferrin TE. A geometric approach to macromolecule–ligand interactions. J Mol Biol. 1982;161(2):269–288.

Macdonald IR, Martin E, Rosenberry TL, Darvesh S. Probing the Peripheral Site of Human Butyrylcholinesterase. Biochemistry. 2012;51:7046-7053.

March RE, Lewars EG, Stadey CJ, Miao X-S, Zhao X, Metcalfe CD. A comparison of flavonoid glycosides by electrospray tandem mass spectrometry. Int J Mass Spectrom. 2006;248(1-2):61–85.

March RE, Miao X-S. A fragmentation study of kaempferol using electrospray quadrupole time-of-flight mass spectrometry at high mass resolution. Int J Mass Spectrom. 2004;231(2-3):157-167.

Morais LCSL, Barbosa-Filho JM, Almeida RN. Central depressant effects of reticuline extracted from *Ocotea duckei* in rats and mice. J Ethnopharmacol. 1998;62(1):57-61.

Nawaz SA, Ayaz M, Brandt W, Wessjohann LA, Westermann B. Cation-pi and pi-pi stacking interactions allow selective inhibition of butyrylcholinesterase by modified quinine and cinchonidine alkaloids. Biochem Biophys Res Commun. 2011;404(4):935-940.

Othman WNNW, Liew SY, Khaw KY, Murugaiyah V, Litaudon M, Awang K. Cholinesterase inhibitory activity of isoquinoline alkaloids from three *Cryptocarya species* (Lauraceae). Bioorg Med Chem. 2016;24(18):4464-4469.

Nelder JA, Mead R. A simplex-method for function minimization. Computer Journal 1965;7:308-313.

Reid GA, Chilukuri N, Darvesh S. Butyrylcholinesterase-Knockout reduces brain deposition of fibrillar β-amyloid an Alzheimer mouse model. J Neurosci Res. 2015;298:424–435.

Salleh WMNHW, Ahmad F. Phytochemistry and Biological Activities of the Genus *Ocotea* (Lauraceae): A Review on Recent Research Results (2000-2016). J Appl Pharm Sci. 2017;7(5):204-218.

Schmidt J, Raith K, Boettcher C, Zenk MH. Analysis of benzylisoquinoline-type alkaloids by electrospray tandem mass spectrometry and atmospheric pressure photoionization. EJMS. 2005;11(3):325-333.

Shoichet BK, Kuntz ID, Bodian DL. Molecular docking using shape descriptors. J. Comput Chem. 1992;13(3):380–397.

Tachakittirungrod S, Okonogi S, Chowwanapoonpohn S. Study on antioxidant activity of certain plants in Thailand: mechanism of antioxidant action of guava leaf extract. Food Chem. 2007;103(2): 381–388.

Tan WN, Khairuddean M, Wong KC, Khaw KY, Vikneswaran M. New cholinesterase inhibitors from *Garcinia atroviridis*. Fitoterapia. 2014;97:261–267.

Tsimogiannis D, Samiotaki M, Panayotou G, Oreopoulou V. Characterization of flavonoid subgroups and hydroxy substitution by HPLC-MS/MS. Molecules. 2007;12(3):593-606.

Ui-Haq Z, Khan W, Kalsoom S, Ansari FL. *In silico* of the specific inhibitory potential of thiophene-2,3dihydro-1,5-benzothiazepine against BChE in the formation of β-amyloid plaques associated with Alzheimer's disease. Theor Biol Med Model. 2010;7:1-26.

Vinutha B, Prashanth D, Salma K, Sreeja SL, Pratiti D, Padmaja R, et al. Screening of selected Indian medicinal plants for acetylcholinesterase inhibitory activity. J Ethnopharmacol. 2007;109(2):359-363.

Vukics V, Guttman A. Structural characterization of flavonoid glycosides by multi-stage mass spectrometry. Mass Spectrom Rev. 2010;29(1):1-16.

Xie Y, Yang W, Chen X, Xiao J. Inhibition of flavonoids on acetylcholine esterase: binding and structure-activity relationship. Food Funct. 2014;5(10):2582-9.

Yan R, Wang W, Guo J, Liu H, Zhang J, Yang B. Studies on the Alkaloids of the Bark of *Magnolia officinalis*: Isolation and On-line Analysis by HPLC-ESI-MS[n]. Molecules. 2013;18(7):7739-7750.

Yang J, Roy A, Zhang Y. Protein-ligand binding site recognition using complementary binding-specific substructure comparison and sequence profile alignment. BMC Bioinformatics. 2013;29(20):2588–2595.